Optical and electronic solutions for power stabilization of CO_2 lasers

Christian Childs, William O'Donnell, Paul B. Ellison, et al.

View Online   Export Citation   CrossMark

ARTICLES YOU MAY BE INTERESTED IN

Optical and electronic solutions for power stabilization of CO₂ lasers

Christian Childs,[a] ⓘD William O'Donnell, Paul B. Ellison, ⓘD David P. Shelton, ⓘD and Ashkan Salamat[b] ⓘD

AFFILIATIONS

Department of Physics and Astronomy, University of Nevada Las Vegas, Las Vegas, Nevada 89154, USA

[a] Author to whom correspondence should be addressed: christianmchilds10@gmail.com
[b] Electronic mail: salamat@physics.unlv.edu

ABSTRACT

High pressure–temperature conditions can be readily achieved through the laser-heated diamond anvil cell (LH-DAC). A stable laser source is required for reliable *in situ* measurements of the sample, as the sample is small with a thermal time constant of the order of microseconds. Here, we show that the power instabilities typical of CO₂ gas lasers used in LH-DAC's are ±5% at the second timescale and ~±50% at the microsecond timescale. We also demonstrate that the pointing instability of the laser requires either a diffuser or an integrating sphere for reliable total power measurements with small sized detectors. We present a simple solution for stabilizing the power of a CO₂ gas laser on the second timescale by the direct modulation of the current across the tube and another solution that stabilizes the power to the microsecond timescale by externally modulating the CO₂ laser beam. Both solutions can achieve a ±0.3% power stability.

Published under license by AIP Publishing. https://doi.org/10.1063/5.0021156

I. INTRODUCTION

Laser beam heating is often used to achieve high sample temperatures in high pressure material science research using diamond anvil cells (DAC), but reliable thermodynamic measurements require a steady state during the measurement time. Due to the small sample size (ng to μg) in diamond anvil cell work, the thermal response time of the sample is of the order of microseconds,[1–5] and steady laser beam power is required to avoid making measurements averaged over a wide temperature range. For many materials that are transparent in the near infrared, laser beam heating using a CO₂ laser operating around 10 μm has an advantage over high power solid state lasers operating near 1 μm since the mid-IR radiation is directly absorbed by the sample and a separate absorber is not needed. This work presents solutions to problems special to power stabilization of a CO₂ laser.

There are many causes for power fluctuations in gas lasers, including pump power variation, mechanical vibrations, and resonator cavity thermal expansion. These effects typically produce fluctuations on the timescale of seconds. However, radiofrequency (RF) excited CO₂ lasers typically use the pulse width modulation (PWM) of the current across the tube to control the average laser power and have large output power fluctuations at microsecond

timescales. A typical PWM frequency is about 5 kHz –20 kHz (2000 μs–50 μs period), and a typical CO₂ laser decay time of around 500 μs–100 μs results in large laser output power changes during the PWM cycle. For small samples typical in a diamond anvil cell (DAC), the thermal time constant is of the order of microseconds,[1,3,4] so the sample temperature will follow the laser output power oscillation. Therefore, even though one would visually observe a steady glow, pyrometric temperature measurements of the sample would be an average of the sample's temporal thermal emission spectra, similar to pulsed laser heating temperature measurements.[1,2,6] Thus, the measured temperature is likely less than the actual peak temperature of the sample and more than the average sample temperature (the intensity is proportional to T^4).

Most (if not all) high pressure research has been done with such modulated RF CO₂ lasers while taking thermal emission measurements for temperature determination.[7–14] It is ideal to either run the laser at near full duty cycle and externally modulate the laser beam or run the laser at high enough modulation frequency (~20 kHz to 100 kHz) such that the laser decay time (typ. 50 μs–100 μs) is long compared to the PWM period.

There have been fewer works stabilizing the CO₂ laser power output compared to the amount of work on stabilizing the lasing frequency of CO₂ gas lasers. There are at least 36 lines from 9 μm

to 11 μm that the CO_2 laser can lase at,[15] and there have been many different ways of stabilizing the CO_2 laser frequency,[16] using methods such as the opto-galvanic effect,[17] saturated absorption spectroscopy,[18] Lamb-dip method,[19] photoacoustic effect,[20–22] and using a Stark cell.[23]

Various methods have been implemented to establish power stabilization in CO_2 gas lasers for heating and metrology. Such methods utilize either internal or external modulation. Internal modulation is the direct modulation of current across the tube or changes to the lasing cavity,[16,20] and external modulation is the modulation of the laser beam after it has left the laser. The simplest and most direct solution is internal modulation by the direct modulation of tube current. However, running the laser at full power and then externally modulating the laser power reaching the experiment have the added benefit of not having significant microsecond fluctuations. Some external modulation methods can include polarization modulation, phase modulation, electro-optic modulation, and electro-absorption modulation.

In this work, we tested two solutions: a direct feedback control method that varies the duty cycle of the current across the laser tube and an external modulation method using a wire-grid polarizer (WGP) on a motorized rotation stage. A small thermopile is used to produce the feedback signal, keeping the response time under 100 ms. An InAsSb photodiode was used to look at the CO_2 laser power output at the microsecond timescale. The direct feedback is a cheaper and simpler solution; however, external modulation has the advantage that it can eliminate the audio frequency laser power oscillation. Synrad offers a CO_2 laser power "closed loop stabilization kit"[24] that stabilizes the power only on the second timescale by varying the duty cycle of the current across the tube. It claims a ±2% stability, while this work and other works using similar methods report a stability of ±0.3%.[25] In this study, we also demonstrate that by running the laser at full duty cycle and externally modulating the power through polarization, we can achieve stability at both second and microsecond timescales.

II. MID-IR DETECTORS

Gas lasers operating in the visible and near-IR range are typically power stabilized by varying the current across the tube while sampling a portion of the beam to a standard silicon photodiode. This becomes more challenging for CO_2 lasers operating primarily at 10.6 μm. These wavelengths in the mid-IR (3 μm–50 μm ISO 20473:2007) are not detectable with common photodiodes. Thus, thermopiles or tailored semiconductors have been used to measure the beam power at these wavelengths.[26] While thermopiles are much more cost effective than mid-IR photodetectors, the thermopiles have a much slower response time (100 ms to 3 s) than photodiodes (~ns). The thermopile's response time depends primarily on the size of the absorber and its thermal time constant. Other high cost detectors include photon drag detectors[27–32] and thermoelectric thin film sensors.

An electronic feedback mechanism that relies on a silicon photodiode sampling the thermal emission of the sample in a DAC has also been utilized in other works.[33–35] The feedback loop would keep the thermal emission of the sample constant by varying the power of the laser.

Semiconductor based photodetectors have response times on the order of electronic timescales, while thermopiles have response times from hundreds of ms to seconds. While a semiconductor photodetector is desirable, for mid-IR radiation, this requires a very small bandgap (~0.1 eV at 10 μm). Thus, it becomes desirable for the detector to be at temperatures much colder than room temperature in order to depopulate the conduction band of the semiconductor for improved signal to noise. $Hg_{1-x}Cd_xTe$ has a tunable bandgap depending on the amount of cadmium in the zincblende structure (replacing Hg).[36,37] Typical HgCdTe detectors are several orders of magnitude higher cost than thermopiles. Likewise, $InAs_{1-x}Sb_x$ has a bandgap tunable by varying the x stoichiometry parameter. For x > 0.61, the increase of Sb adds a strain to the Zinc-blende lattice, which lowers the bandgap to the 8 μm–12 μm range.[38]

In this study, a ZTP-315 thermopile from Amphenol Advanced Sensors ($4.33 each from mouser.com) is used to measure the average power of the laser. The thermopile has an optical filter passing 5 μm–14 μm and has a 25 ms time constant. The measured response time using a 125 Hz bandwidth amplifier was 86 ± 1 ms (1/e). The thermopile outputs a voltage proportional to the temperature difference between the absorber and the case. The case temperature can be measured via a thermistor attached to the case.
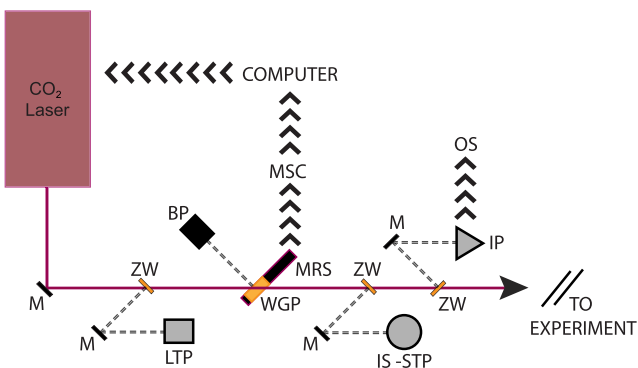
An InAsSb photodetector was purchased from Hamamatsu (model No. P13894) for its fast response (<10 ns rise time). The photodetector was operated uncooled with zero bias across the photodiode (photovoltaic detector), connected to a first gain stage comprised of an AD8638 op-amp configured as a trans-impedance amplifier (current to voltage converter). The P13894 photovoltaic detector has a shunt resistance around 2 kΩ at room temperature, so we chose 2 kΩ for our feedback resistor. A 100 pF capacitor was placed in parallel with the 2 kΩ resistor for a bandwidth of about 700 kHz. The output of the first stage is fed into the second stage for amplification. The second gain stage is comprised of a high speed dual op-amp (ADA4625-2). To save time, we used the EVAL-ADA4625-2ARDZ demo board and configured it as two identical cascaded amplifiers each with a gain of 10. The feedback network (1.82 kΩ in parallel with a 100 pF) yields a bandwidth of about 700 kHz for each amp. With the three amplifiers cascaded together, the system bandwidth is about 400 kHz (2.5 μs response).

III. LASER SPATIAL INTENSITY STABILITY

In order to keep the response time of the thermopile low, we used a small thermopile (1.3 × 1.3 mm^2 active area). With the beam focused onto the thermocouple's active area, we found large deviations of the thermopile signal compared to the signal from a larger thermopile monitoring the same beam. It was determined that the spatial intensity distribution of the laser beam varied with time, resulting in an erratic signal from the small thermopile.

To solve this issue, a custom-made integrating sphere was used to integrate over the beam's spatial profile. A 2 in. spherical cavity was machined in a stainless steel block, and the inner surface of the sphere was bead blasted to make the surface nearly Lambertian. Gold was electro-plated onto the bead blasted surface to enhance mid-IR reflectivity. The laser light was directed off the center of the sphere through an entrance hole placed off of the equator of the sphere containing the exit hole and thermopile, ensuring that any specular

FIG. 1. The full power stabilization circuit for a CO$_2$ laser using external modulation by polarization. The various components are labeled as follows: M—mirror, ZW—ZnSe window, BP—beam dump, WGP—wire-grid polarizer, MRS—motorized rotation stage, MSC—motorized stage controller, LTP—large thermopile, IS-STP—integrating sphere with small thermopile, IP—InAsSb photovoltaic, and OS—oscilloscope.

reflections of the beam entering the entrance hole do not immediately exit through the exit hole or back out the entrance hole. The area of the entrance hole was kept small (1/4 in. diameter) compared to the area of the sphere to homogeneously average the input signal (0.4%). The exit hole diameter was matched to the casing of the thermopile.

The integrating sphere solved the thermopile signal issue, and the signal from the small thermopile matched the signal of a large thermopile. A simple reflective diffuser may solve this issue as well.

IV. MODULATION OF THE CO$_2$ LASER POWER

A Synrad Evolution 100 W CO$_2$ laser was used to measure the power output stability. Figure 1 shows the optical setup for external modulation. For the internal modulation experiment, the setup is the same except the WGP and large thermopile are removed. About <0.5% of the laser power is picked off by an AR-coated ZnSe window (Thorlabs WW71050-E3) and sent to the integrating sphere and thermopile. Both thermopiles were connected to a data acquisition device (NI USB-6341) and monitored using LabVIEW. Another ZnSe window picks off a small portion of the beam and sends it to the InAsSb detector and oscilloscope for measuring the laser beam power profile at the microsecond timescale.

Figure 2 shows the instability of a CO$_2$ laser (solid black line) and the stabilized output (solid red line) for both the internal and external modulation. The top graph shows the direct modulation of the CO$_2$ laser, while the bottom graph shows the external modulation using a WGP. At t = 0 s, the laser is turned on to 35% or 40% duty cycle and left alone for about 180 s. At t = 180 s, the laser is turned off. Both methods are viable, keeping the stability of the laser to 0.3%. The limiting factor of greater stability is simply the noise of the thermopile. A detector with higher signal to noise would improve stability further.

The oscillations of the CO$_2$ laser power shown in Fig. 2 are due to cavity thermal expansion as the laser warms up after the RF pump power is turned on. At the typical operating gas pressure of 100 Torr, the pressure broadened gain bandwidth for a CO$_2$ molecular rotation-vibration laser transition is about 750 MHz. For a 1 m laser cavity, the longitudinal mode spacing is 150 MHz, and several resonator modes will fall within the narrow CO$_2$ laser gain band. Mode competition in such a homogeneously broadened gain medium tries to enforce single longitudinal mode operation, but spatial hole burning allows two or more lasing modes to coexist. The thermal expansion of the resonator causes the mode frequencies to sweep across the gain curve, and the extracted power varies as the gain for each
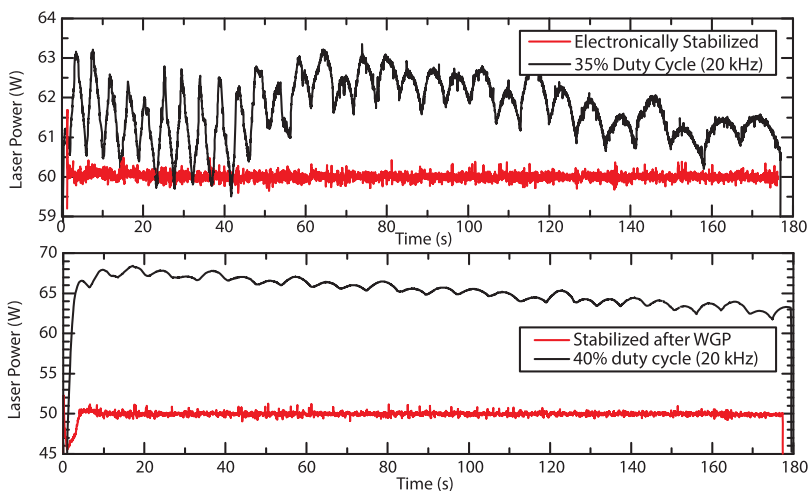
FIG. 2. The raw CO$_2$ laser power (solid black) and the stabilized output using direct modulation (top) and a wire-grid polarizer (bottom) of Synrad Evolution 100. The direct modulation was taken after the raw output instability was measured (two separate runs). The error in the power measurement is equivalent to the shot noise of the thermopile, which is ±0.3 W. The response time of the detector is fast (86 ± 1 ms) compared to the scale of the x-axis. The WGP method used two different thermopiles to measure the instability and stabilized beam on a single 180 s run.

lasing mode varies as it moves across the gain curve. The periodicity of the resonator modes results in periodic power fluctuation due to mode sweeping, which slows down as the rate of change of cavity temperature and length decreases.

The laser has predominantly TEM_{00} mode output ($M^2 = 1.2$). A small admixture of another transverse mode can also vary with mode sweeping, and this may account for the excess signal variation seen by the fast thermopile without the integrating sphere, as discussed in Sec. III.

A. Direct modulation

For direct modulation, the duty cycle is varied according to the integrating sphere and fast thermopile feedback signal. The LabVIEW code was written with a proportional–integral–derivative (PID) algorithm to send a 0 V–10 V signal to the laser controller (Synrad UC2000). This laser controller varies the PWM duty cycle of the current across the laser tube depending on the 0 V–10 V signal.

The response shown in red in Fig. 2 (top) is obtained with the direct modulation of the CO_2 laser current. At t = 0 s, the set point was set to 60 W, and then at t = 180 s, the set point was changed to 0 W. Feedback control reduces the fluctuations from ±2.5% to ±0.3%. This stability at the second timescale is sufficient for most applications; however, the power will still suffer from the microsecond timescale fluctuations shown in Fig. 3.

B. External modulation by polarization

A method commonly used for externally stabilizing the power output utilizes the linearly polarized output of most lasers. Gas lasers typically have their laser cavity windows set at Brewster's angle, leading to a polarized output. Taking advantage of this polarization, one could add a variable polarizer to vary the transmitted laser power. A variable polarizer can take many forms, such as half-wave plate and polarizer, Pockels cell and polarizer, or polarizer on a rotation stage. Birefringent crystal half-wave plates for mid-IR are an order of magnitude more costly than visible half-wave plates, but multilayer thin film retarders are an alternative.[39] Types of polarizers used in the mid-IR include a wire grid coated on a transparent window (e.g., ZnSe) or a series of transparent windows set at Brewster's angle.[40]

An electro-optical modulator (EOM) for 10 μm light is possible using a Pockels cell, which would require a single crystal material with a high electro-optical coefficient. CdTe is transparent to the mid-IR (bandgap = 1.5 eV), is birefringent, and has the highest linear electro-optical coefficient of the II–VI compounds.[41,42] Applying an electric field by a capacitor across an electro-optical single crystal will change the index of refraction parallel to that axis. Orienting the crystal and capacitor at a 45° to the laser will result in a variable wave plate.[42] The response time is only limited by the ability to charge the capacitor (~ns). A Pockels cell may be worth the cost depending on the needs of the experiment.

To stabilize the power density of the laser at the region of interest, a wire-grid polarizer (WGP) (Edmund Optics No. 62-772) is deployed to externally modulate the power of the laser output. The WGP is mounted on a motorized rotation stage (Thorlabs PRM1Z8). The WGP reflects a portion of the laser beam into a beam dump depending on the angle of the polarizer relative to the polarization of the beam. At high laser power densities (≥ 50 W/cm^2), a
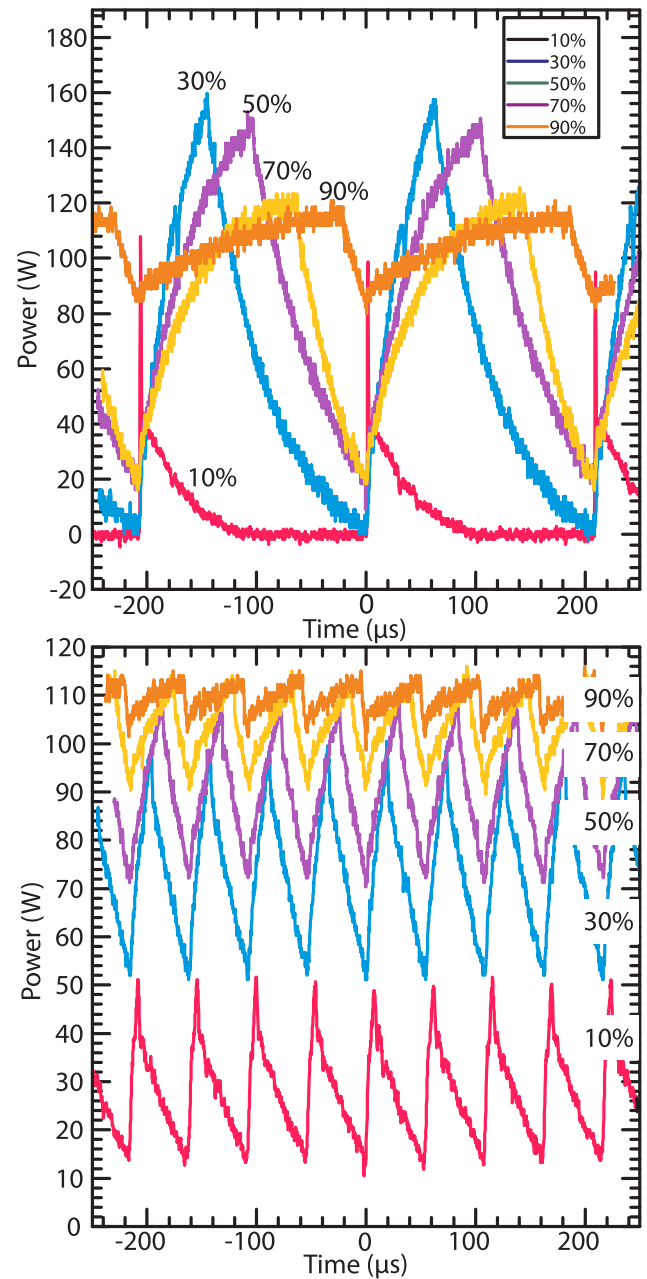
FIG. 3. CO_2 laser power as measured from the InAsSb photovoltaic detector. The system setup is illustrated in Fig. 1. The top graph is at 5 kHz duty cycle, and the bottom graph is at 20 kHz duty cycle. Each line is labeled with its corresponding duty cycle percentage. The shot noise of this detector is ±1 W and represents the error on the measurement. The response time of the detector is much faster (400 kHz, 2.5 μs) than the x-axis scale of this graph.

visible change to the wire grid was observed where the CO_2 laser passed through. The visible discoloration on the wire grid did not appear to affect the polarizing ability of the wire-grid. This is likely due to the wire-grid polarizer not being rated for these high power
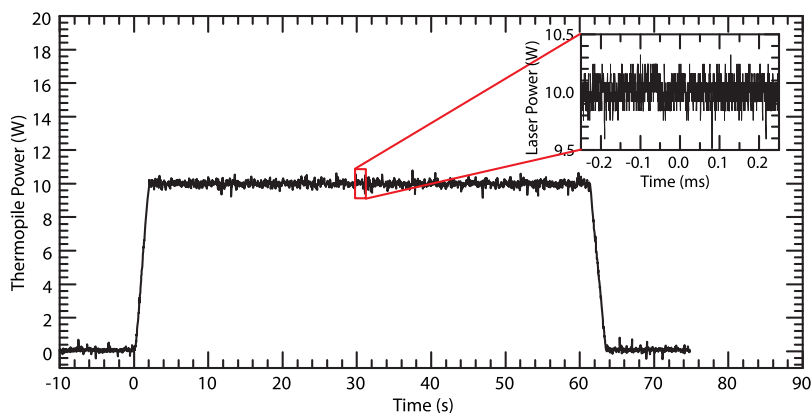
FIG. 4. The results from running the CO_2 laser at 100% duty cycle and externally modulating the laser power using a wire-grid polarizer on a rotation stage. Figure 1 illustrates the experimental setup. The main graph is the stabilized output, as measured from the integrating sphere and fast thermopile. The inset is the measurement from the InAsSb photovoltaic detector.

densities, and future experiments should be designed with wire-grid polarizers rated for such high laser power densities. A LabVIEW code with a PID algorithm was written to keep the integrating sphere and small thermopile signal constant by sending the motorized rotation stage a varying duty cycle that varied the rotation speed of the WGP.

The bottom of Fig. 2 shows the signal from the integrating sphere and small thermopile, measuring the CO_2 laser beam power with WGP stabilization (solid red line). The solid black line is the large thermopile signal. At t = 0 s, the set point was set to 50 W. At around t = 150 s, the laser was turned off. The fluctuations are reduced from ±2.5% to ±0.3%. This stability at the second timescale is sufficient for most applications; however, the microsecond timescale fluctuations that are shown in Fig. 3 will remain. In order to also gain stability at the microsecond timescale, we ran the laser at full duty cycle and then externally modulated the laser power.

V. MICROSECOND LASER POWER FLUCTUATIONS

Figure 3 shows the CO_2 laser power as measured by the InAsSb detector. The top graph is the power output for 5 kHz PWM, and the bottom graph is for 20 kHz PWM. For 5 kHz modulation at up to 30% duty cycle, the laser power returns all the way back to zero for part of each cycle, which will lead to extreme temperature variations in a sample in a DAC. Even at 20 kHz, the oscillations are as much as ±50% at 10% duty cycle. Fitting to both the decay and rise of the laser for 5 kHz PWM at 50% duty cycle, we get a rise time constant of 54 ± 1 μs and a decay time constant of 73 ± 2 μs for the Synrad Evolution 100 W CO_2 laser. With a typical thermal time constant of 10 μs for a sample in a laser-heated diamond anvil cell (LH-DAC), the sample will follow these laser power fluctuations closely. It is clear that in order to take accurate *in situ* measurements at high temperatures, these fluctuations must be eliminated.

To resolve this issue, we run the laser at 100% duty cycle and externally modulate the CO_2 beam through polarization. Figure 4 shows the result of this experiment. The main graph shows the stabilized output from the thermopile, while the inset shows the laser power measured from the InAsSb photovoltaic detector. The stability of the laser is seen to only be limited by the shot noise of the detector.

VI. APPLICATIONS FOR HIGH PRESSURE STUDIES

The temporal instabilities that we measure are relevant over timescales relevant for thermalization and have a significant influence on measurements using CO_2 laser heating in the diamond anvil cell for studies at high pressure–temperature conditions. These effects of inherent power instability cannot be ignored and must be addressed in the future studies. The ability to directly couple the 10.6 μm CO_2 laser beam with low Z molecular systems like water-ice and ammonia permits high temperatures to be generated in the diamond anvil cell. With improvements in the laser power stability, a more quantifiable set of studies can be undertaken to further our understanding of the complex chemical processes deep in the planet interiors. This, in turn, requires accurate measurements of a H–C–N–O multi-component phase diagram under high pressure/temperature conditions.[43] At more modest conditions of a few GPa and hundreds of kelvins, these chemical systems play a different and yet dominating role in smaller bodies such as the moons of the Jovian-giants and orbiting planetesimals/comets.[44] Many of the large Jovian icy moons contain water ice, mixed with volatiles such as CH_4, and CO_2 and ionic salt species.[45] With CO_2 laser power stability established, a more reliable route is possible for precise measurements pertaining to the interior of water-rich exoplanets and varying synthetic Uranus recipes.

VII. CONCLUSION

Two methods were used to stabilize the power of a CO_2 laser: a direct modulation of the duty cycle and an external modulation by polarization. Direct modulation is the simplest method; however, oscillations of the CO_2 laser beam power at the PWM frequency will be present. External modulation by a wire-grid polarizer is a viable method for low power densities (<50 W/cm^2). Both methods keep the slow fluctuations within the noise of the detector used (~0.3 W). External modulation, when used with constant laser current (PWM with 100% duty cycle), also gives stability on the μs timescale by eliminating the fast laser power switching transients due to PWM.

Further improvement in stabilization is possible by using a detector with less noise. The thermopile is a cheap but slow solution, while the photovoltaic detector is more expensive but can respond much more quickly and reliably. The pointing stability of these lasers can lead to a chaotic signal if the detector area is small compared

to the area of the beam. A diffuser or integrating sphere should be used to ensure accurate measurements of the total laser power output.

The power oscillations of a PWM RF CO_2 laser can be extreme. With a sample size typical of those found in a DAC, the resulting sample temperature oscillation will be similar to the pattern seen in Fig. 3. It is vital in high pressure research to resolve this issue in order to take accurate temperature and other *in situ* measurements. One method of resolving this issue was demonstrated by running the laser at full duty cycle and externally modulating the laser power through polarization. Comparing Fig. 4 to Fig. 3, it is seen that this method of running the laser at full duty cycle and externally modulating the CO_2 laser beam stabilizes the laser beam down to the microsecond timescale. Faster oscillations than the microsecond timescale may be present but are not a concern for samples with a thermal time constant of ≥ 10 μs, as are seen in diamond anvil cell experiments. In this study, a WGP was used; however, due to the high energy densities of the laser, it would be more robust to use a polarizer with a high damage threshold, such as a thin film plate polarizer or a series of windows (ZnSe or Ge) set at Brewster's angle.

ACKNOWLEDGMENTS

DATA AVAILABILITY

The data that support the findings of this study are available within the article.

REFERENCES

[1]S. Rekhi, J. Tempere, and I. F. Silvera, "Temperature determination for nanosecond pulsed laser heating," Rev. Sci. Instrum. **74**, 3820–3825 (2003).

[2]S. Deemyad, E. Sterer, C. Barthel, S. Rekhi, J. Tempere, and I. F. Silvera, "Pulsed laser heating and temperature determination in a diamond anvil cell," Rev. Sci. Instrum. **76**, 125104 (2005).

[3]S. Petitgirard, A. Salamat, P. Beck, G. Weck, and P. Bouvier, "Strategies for *in situ* laser heating in the diamond anvil cell at an X-ray diffraction beamline," J. Synchrotron Radiat. **21**, 89–96 (2014).

[4]Z. M. Geballe, G. W. Collins, and R. Jeanloz, "Modulation calorimetry in diamond anvil cells. I. Heat flow models," J. Appl. Phys. **121**, 145902 (2017).

[5]M. Zaghoo, A. Salamat, and I. F. Silvera, "Evidence of a first-order phase transition to metallic hydrogen," Phys. Rev. B **93**, 155128 (2016).

[6]S. Deemyad, A. N. Papathanassiou, and I. F. Silvera, "Strategy and enhanced temperature determination in a laser heated diamond anvil cell," J. Appl. Phys. **105**, 093543 (2009).

[7]J. A. Queyroux, S. Ninet, G. Weck, G. Garbarino, T. Plisson, M. Mezouar, and F. Datchi, "Melting curve and chemical stability of ammonia at high pressure: Combined x-ray diffraction and Raman study," Phys. Rev. B **99**, 134107 (2019).

[8]D. Andrault, G. Morard, G. Garbarino, M. Mezouar, M. A. Bouhifd, and T. Kawamoto, "Melting behavior of SiO_2 up to 120 GPa," Phys. Chem. Miner. **47**, 10 (2020).

[9]T. Kimura, H. Ohfuji, M. Nishi, and T. Irifune, "Melting temperatures of MgO under high pressure by micro-texture analysis," Nat. Commun. **8**, 15735 (2017).

[10]T. Kimura, Y. Kuwayama, and T. Yagi, "Melting temperatures of H_2O up to 72 GPa measured in a diamond anvil cell using CO_2 laser heating technique," J. Chem. Phys. **140**, 074501 (2014).

[11]A. Kurnosov, H. Marquardt, L. Dubrovinsky, and V. Potapkin, "A waveguide-based flexible CO_2-laser heating system for diamond-anvil cell applications," C. R. Geosci. **351**, 280–285 (2019).

[12]K. Brister and W. Bassett, "CO_2 laser heating instrumentation at CHESS," Rev. Sci. Instrum. **66**, 2698–2702 (1995).

[13]G. Fiquet, D. Andrault, A. Dewaele, T. Charpin, M. Kunz, and D. Haüsermann, "P-V-T equation of state of $MgSiO_3$ perovskite," Phys. Earth Planet. Inter. **105**, 21–31 (1998).

[14]A. Dewaele, G. Fiquet, D. Andrault, and D. Hausermann, "P-V-T equation of state of periclase from synchrotron radiation measurements," J. Geophys. Res.: Solid Earth **105**, 2869–2877, https://doi.org/10.1029/1999jb900364 (2000).

[15]J. Reid and K. Siemsen, "New CO_2 laser bands in the 9–11-μm wavelength region," Appl. Phys. Lett. **29**, 250–251 (1976).

[16]M. W. Lund, J. N. Cogan, and J. A. Davis, "Low-cost method for stabilization of a CO_2 laser for use in far infrared laser pumping," Rev. Sci. Instrum. **50**, 791–792 (1979).

[17]S. Moffatt and A. L. S. Smith, "High frequency optogalvanic signals and CO_2 laser stabilisation," Opt. Commun. **37**, 119–122 (1981).

[18]B. Frech, L. F. Constantin, A. Amy-Klein, O. Phavorin, C. Daussy, C. Chardonnet, and M. Mürtz, Appl. Phys. B **67**, 217–221 (1998).

[19]V. P. Kochanov, S. P. Belov, and G. Y. Golubiatnikov, "Lamb dip spectroscopy with the use of frequency-modulated radiation," J. Quant. Spectrosc. Radiat. Transfer **149**, 146–157 (2014).

[20]R. Huang, X. Guo, Q. Meng, and B. Zhang, "A simple digital control system with field-programmable gate array for stabilization of CO_2 laser output," Rev. Sci. Instrum. **88**, 043105 (2017).

[21]J. Choi, "Frequency stabilization of a radio frequency excited CO_2 laser using the photoacoustic effect," Rev. Sci. Instrum. **81**, 064901 (2010).

[22]L. Wang, Z. Tian, Y. Zhang, J. Wang, S. Fu, J. Sun, and Q. Wang, "Frequency stabilization of pulsed CO_2 laser using setup-time method," Chin. Opt. Lett. **10**, 011402 (2012).

[23]K. Nakayama, S. Okajima, T. Akiyama, K. Tanaka, and K. Kawahata, "Stabilization of 48- and 57-μm CH_3 OD lasers for plasma diagnostics," J. Instrum. **10**, C12002 (2015).

[24]Closed Loop Kit|Synrad.

[25]M. A. Jebali, "Polarization and wavelength insensitive optical feedback control systems for stabilizing CO_2 lasers," Proc. SPIE **9730**, 97301C (2016).

[26]P. L. Richards, "Bolometers for infrared and millimeter waves," J. Appl. Phys. **76**, 1–24 (1994).

[27]B. S. Patel, "Photon-drag germanium detectors for CW CO_2 lasers," Proc. IEEE **62**, 143–144 (1974).

[28]A. F. Gibson and A. C. Walker, "Sign reversal of the photon drag effect in p-type germanium," J. Phys. C: Solid State Phys. **4**, 2209–2219 (1971).

[29]A. F. Gibson and S. Montasser, "A theoretical description of the photon-drag spectrum of p-type germanium," J. Phys. C: Solid State Phys. **8**, 3147–3157 (1975).

[30]M. F. Kimmitt, "Detection of infrared, free-electron laser radiation," Proc. SPIE **1501**, 86 (1991).

[31]M. F. Kimmitt, D. C. Tyte, and M. J. Wright, "Photon drag radiation monitors for use with pulsed CO_2 lasers," J. Phys. E: Sci. Instrum. **5**, 239–240 (1972).

[32]S. D. Alaruri, "Construction of a photon drag detector for evaluating the performance of a CO_2 laser amplifier," Optik **125**, 4964–4967 (2014).

[33]R. Boehler, "Laser heating in the diamond cell: Techniques and applications," Hyperfine Interact. **128**, 307–321 (2000).

[34]R. Boehler and A. Chopelas, "A new approach to laser heating in high pressure mineral physics," Geophys. Res. Lett. **18**, 1147–1150, https://doi.org/10.1029/91gl01144 (1991).

[35]G. Serghiou, A. Zerr, L. Chudinovskikh, and R. Boehler, "The coesite–stishovite transition in a laser-heated diamond cell," Geophys. Res. Lett. **22**, 441–444, https://doi.org/10.1029/94gl02692 (1995).

[36] G. L. Hansen, J. L. Schmit, and T. N. Casselman, "Energy gap versus alloy composition and temperature in $Hg_{1-x}Cd_xTe$," J. Appl. Phys. **53**, 7099–7101 (1982).

[37] P. Norton, "HgCdTe infrared detectors," Opto-Electronics Rev. **10**(3), 159–174 (2002).

[38] G. C. Osbourn, "InAsSb strained-layer superlattices for long wavelength detector applications," J. Vac. Sci. Technol., B **2**, 176 (1984).

[39] H. Nishi, H. Iwamoto, N. Ujiie, and K. Yajima, "Transparent waveplate (retarder) of ZnSe for high power CO_2 lasers," SEI Tech. Rev. **81**, 72–76 (2015).

[40] D. J. Dummer, S. G. Kaplan, L. M. Hanssen, A. S. Pine, and Y. Zong, "High-quality Brewster's angle polarizer for broadband infrared application," Appl. Opt. **37**, 1194–1204 (1998).

[41] D. B. Chenault, R. A. Chipman, and S.-Y. Lu, "Electro-optic coefficient spectrum of cadmium telluride," Appl. Opt. **33**, 7382 (1994).

[42] G. L. Herrit and H. E. Reedy, "Measurement of the birefringence in cadmium telluride electro-optic modulators," Proc. SPIE **1307**, 509–516 (1990).

[43] G. Saleh and A. R. Oganov, "Novel stable compounds in the C-H-O ternary system at high pressure," Sci. Rep. **6**, 32486 (2016).

[44] T. Guillot and D. Gautier, "Giant planets," in *Treatise on Geophysics*, 2nd ed. arXiv:0912.2019.

[45] B. Journaux, I. Daniel, S. Petitgirard, H. Cardon, J.-P. Perrillat, R. Caracas, and M. Mezouar, "Salt partitioning between water and high-pressure ices. Implication for the dynamics and habitability of icy moons and water-rich planetary bodies," Earth Planet. Sci. Lett. **463**, 36–47 (2017).